Russian Journal of General Chemistry, Vol. 75, No. 3, 2005, pp. 359–369. Translated from Zhurnal Obshchei Khimii, Vol. 75, No. 3, 2005, pp. 395–405.

An Experimental and Theoretical Study of Intramolecular Cyclization of Phosphorylated Thioureas

V. V. Zverev,* G. A. Chmutova, M. A. Pudovik,* N. A. Khailova,* R. Kh. Bagautdinova,* N. M. Azancheev,* I. A. Litvinov,* O. N. Kataeva,* and A. N. Pudovik***

**Arbuzov Institute of Organic and Physical Chemistry, Kazan Scientific Center, Russian Academy of Sciences Kazan, Tatarstan, Russia*

***Kazan State University, Kazan, Tatarstan, Russia*

Received June 17, 2003

Abstract — New 1,3,2-thiazaphospholines were prepared, and their steric and electronic structures were examined. The steric and electronic structure of *N*-[(*O*-methyl)chloromethylthiophosphoryl]thiourea and the pathways of their intramolecular cyclization and rearrangement were studied by *ab initio* and semiempirical methods. The influence exerted by the conformational factors in thiourea and in the anion formed from it under the conditions of base catalysis on the direction of the reactions involving these species was revealed, and the structure of intermediate complexes and the final products was determined.

Recently we developed a new route to polyheterocyclic phosphorus derivatives containing endocyclic P–C bonds. It is based on intramolecular transformations of polyfunctional derivatives of four-coordinate phosphorus atom bearing haloalkyl groups in combination with other structural fragments [1–3]. In this study, with the aim to expand the synthetic potential of our approach, determine the conditions of cyclization of haloalkylphosphonates, and prepare new types of 1,3,4-oxaza(thiaza)phospholines, we examined the addition of some proton-containing nucleophiles (guanidine, diamines) to chloromethylisothiocyanatidophosphonothioate **I**. Also we studed the intramolecular cyclization of *N*-[(*O*-methyl)chloromethylthiophosphoryl]thiourea by *ab initio* methods in the HF/6-31G* basis set, by the density functional theory (DBT/PBE/TZ2P), and also by semiempirical MNDO and PM3 methods.

We found that tetramethylguanidine reacts with *O*-phenyl chloromethylisothiocyanatidophosphonothioate **I** to form 2-(1,3-tetramethyl)guanidino-4-thioxo-4-phenoxy-Δ^2-1,3,4λ^5-thiazaphospholine **III**. The reaction probably involves formation of phosphorylated thiourea **II**, which undergoes cyclization by intramolecular alkylation of the thiocarbonyl sulfur atom with the chloromethyl group. The structure of 1,3,4-thiazaphospholine **III** was determined by IR and ^{1}H, ^{13}C, and ^{31}P NMR spectroscopy, and the composition was confirmed by elemental analysis. The phosphorus chemical shift (δ_P 118 ppm) in phospholine **III** is typical of compounds of this type. The IR spectrum of **III** contains the absorption bands of exocyclc (1660 cm^{-1}) and endocyclic (1590 cm^{-1}) C=N bonds.

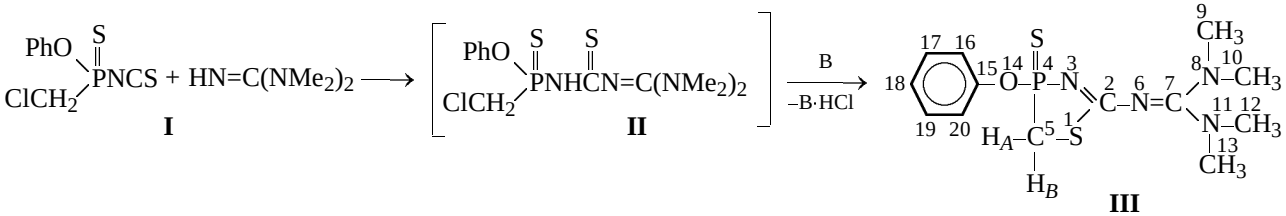

The molecular and crystal structure of 2-(1,3-tetramethyl)guanidino-4-thioxo-4-phenoxy-Δ^2-1,3,4λ^5-thiazaphospholine **III** was determined by single crystal X-ray diffraction. The steric structure of **III** is shown in Fig. 1. The conformation of the five-membered ring of the molecule is a flattened envelope. The S^1, C^2, N^3, and P^4 atoms are coplanar within 0.026(3) Å. The C^5 atom of the methylene group

1070-3632/05/7503-0359

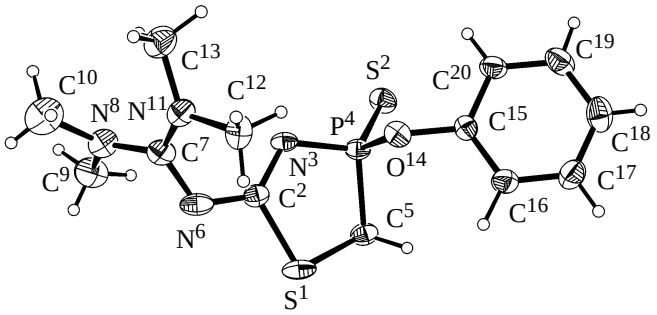

Fig. 1. Steric structure of the independent molecule of **III** in the crystal.

deviates from this plane by 0.349(3) Å. The phenoxy group has a *gauche* conformation relative to the thiophosphoryl bond [$\tau = -45.7(2)°$], and the phenyl ring is perpendicular to the P–O bond. The π-electron systems of the double C=N bonds are strongly delocalized. As a result, the C^2–N^3 and C^2–N^6 bonds are equal within the limits of experimental errors, as well as the C^7–N^8 and C^7–N^{11} bond lengths, and the length of the N^6–C^7 bond is virtually the same as the lengths of the C^7–N^8 and C^7=N^{11} bonds (Table 1). Two planar π systems form a dihedral angle of –57.2(4)°. The molecular geometry is fairly strained. The deviations of the geometric parameters of the molecule (bond angles N^6–C^7–N^{11} and N^3–C^2–N^6) from the "ideal" values are caused by the steric contacts appearing owing to the tendency to delocalization of the electron density in the guanidine moiety. Because of the steric repulsion of the C^{12} atoms from the C^2 and N^3 atoms ($C^{12}\cdots C^2$ 2.97 Å, $C^{12}\cdots N^3$ 3.15 Å), the bond angle $N^6C^7N^{11}$ determining these short contacts increases by 5°. The repulsion between the methyl groups of the neighboring dimethylamino groups is strong, the $C^{10}\cdots C^{13}$ distance is 2.94 Å, and hence the bond angles C^7–N^{11}–C^{13} and C^7–N^8–C^{10} increase (Table 1).

Table 1. Interatomic distances (*d*) and bond angles (ω) of the independent molecule of **III**

Bond	*d*, Å	Angle	ω, deg
P^4–O^{14}	1.610(2)	$P^4O^{14}C^{15}$	122.8(2)
O^{14}–C^{15}	1.403(4)	$N^3P^4C^5$	101.9(1)
P^4–S^2	1.928(1)	$P^4N^3C^2$	114.7(2)
P^4–C^5	1.825(3)	$N^3C^2S^1$	119.2(2)
P^4–N^3	1.628(2)	$C^2S^1C^5$	95.5(1)
S^1–C^2	1.792(3)	$S^1C^5P^4$	105.2(2)
S^1–C^5	1.788(3)	$N^3C^2N^6$	128.3(3)
N^3=C^2	1.311(4)	$S^1C^2N^6$	112.5(2)
N^6=C^2	1.313(4)	$C^2N^6C^7$	119.7(3)
N^6–C^7	1.351(4)	$N^6C^7N^8$	117.3(3)
C^7=N^8	1.343(4)	$N^6C^7N^{11}$	122.3(3)
C^7=N^{11}	1.338(4)	$N^8C^7N^{11}$	120.3(3)
N^8–C^9	1.447(5)	$C^7N^8C^9$	119.7(3)
N^8–C^{10}	1.469(5)	$C^7N^8C^{10}$	122.8(3)
N^{11}–C^{12}	1.442(4)	$C^9N^8C^{10}$	116.1(3)
N^{11}–C^{13}	1.463(4)	$C^7N^{11}C^{12}$	120.1(3)
		$C^7N^{11}C^{13}$	124.6(3)
		$C^{12}N^{11}C^{13}$	113.9(3)

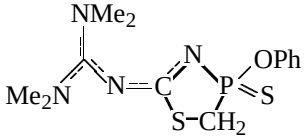

In the crystal, the molecules of **III** are packed in layers, and the interlayer space is filled with the benzene molecules of solvation zene (Fig. 2). No contacts shorter than the sum of the van der Waals radii are observed between the molecules of the main compound and benzene.

As a continuation of our studies, we performed the reactions of **I** with alkylenediamines **IVa** and **IVb**. The initially formed adducts **Va** and **Vb** contain two phosphorylated thiourea fragments, which predetermines the possibility of formation of two 1,3,4-thiazaphospholine rings. The reaction product, *N*,*N*'-bis(4-thioxo-4-phenoxy-Δ^2-1,3,4λ^5-thiazaphospholin-2-yl)propylenediamine **VIb**, is formed as a mixture of four diastereomers in 34 : 21 : 18 : 27 ratio, which is due to the presence of three asymmetric centers (two phosphorus atoms and one carbon atom) in the molecule.

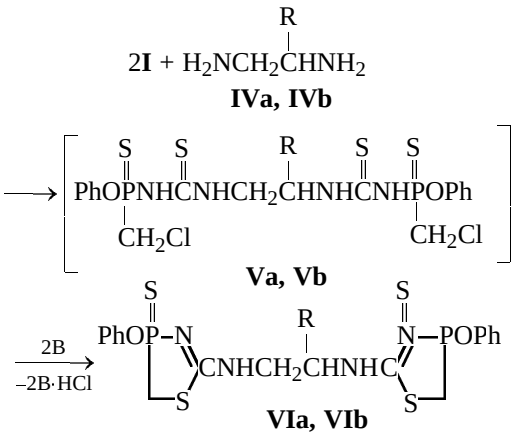

IV–**VI**, R = H (**a**), Me (**b**).

Thus, we found that compounds of the type **VIIa** and **VIIb**, *N*-(chloromethylthiophosphoryl)thioureas, cyclize under the mild conditions in the presence of triethylamine to form 1,4,2-diazaphospholidines **VIII** and (or) 1,3,4-oxaza(thiaza)phospholines **IX** [1–3].

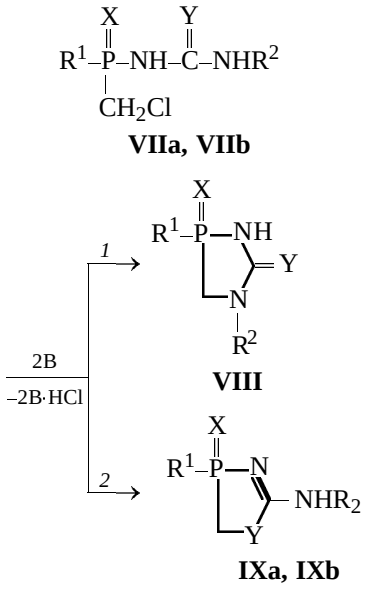

R^1 = OMe, R^2 = H, X = Y = S (**VIIa, IXa**); R^1 = OMe, R^2 = H, X = O, Y = S (**VIIb, IXb**); R^1 = CH_2Cl, CH_3O, C_6H_5O, CH_3; R^2 = H, *t*-Bu, Ph; X, Y = O, S (**VIII**).

Cyclic products of the first type (**VIII**) are the major products in the cyclization of ureas (Y = O), and those of the second type (**IX**), in the cyclization of thio analogs (Y = S). Examination of the thermochemical characteristics of these reactions by the semiempirical MNDO and PM3 methods and by the DFT method [4, 5] has shown that the above reaction pathways are thermodynamically favorable. For phosphorylated ureas **VII** (Y = O), the cyclization pathway was studied by the MNDO method [4]. The shape of the potential energy surface of the cyclization is largely determined by the conformational effect and the presence of the base catalyst. The mechanism of heterocyclization in the presence of phosphorylated thioureas **VIIa** was not theoretically considered previously. Therefore, in this study, using the MNDO, *ab initio* HF/6-31G*, and density functional (DFT/PBE/TZ2P) methods, we examined the possible pathways of cyclization of one of thioureas, **VIIa** (X, Y = S; R^1 = CH_3O; R^2 = H), analyzed the main characteristics of its electonic and steric structure, and evaluated the energy and structure of possible intermediates and activated complexes, and this characterized the potential energy surface for the cyclization of this compound.

Note that all the calculation methods reproduce the main structural characteristics of the cyclic reaction product, 1,3,4-thiazaphospholine **IXa**, in agreement with the X-ray data for the related compounds, 2-(1,1,3,3-tetramethyl)guanidino-4-thioxo-4-phenoxy-Δ^2-1,3,4λ^5-thiazaphospholine **III** considered in this paper and diphenyl *N*-(4-thioxo-4-phenoxy-Δ^2-1,3,4λ^5-thiazaphospholin-2-yl)-*N*-methylamino(phenyl)methylphosphonate studied previously [6]. Table 2 (cf. Table 1) shows that the intracyclic bond angles and the flattened structure of the thiazaphospholine ring are well reproduced. At the same time, the interatomic distances obtained with various calculation methods differ from each other. The values obtained by the Hartree–Fock method are the best consistent with the experiment. In the DFT calculations interatomic distances are systematically overestimated. Inclusion of the polarization and diffuse functions in the basis set in *ab initio* calculations and also consideration of the effects of electronic correlations within the framework of the second-order perturbation theory (MP2) only slightly affect the geometric parameters of the cyclic system.

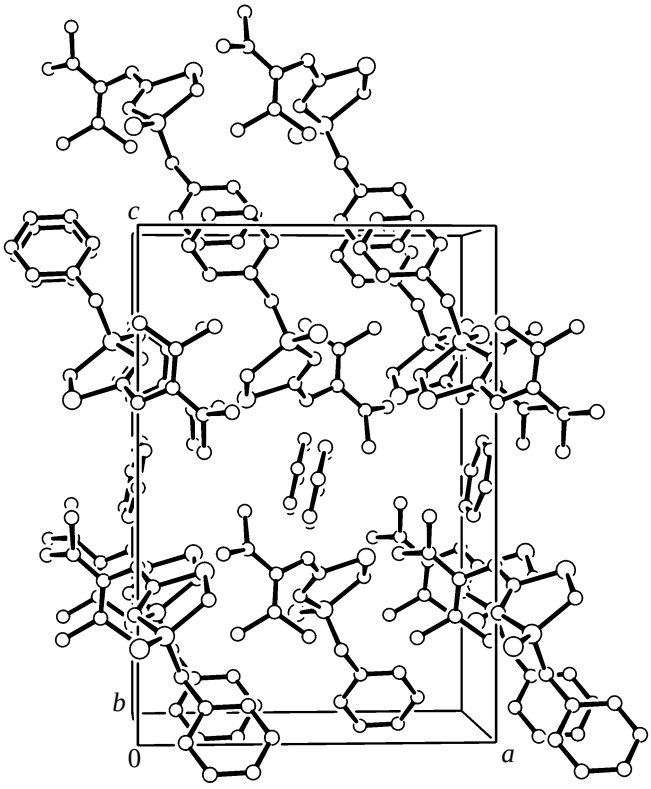

Fig. 2. Packing of the molecules of **III** in the crystal lattice.

Taking into account the complexity of the systems under study, associated with the conformational flexibility of the reactants, reaction products, and possible transition states and intermediates, we paid special attention to the analysis of the steric and electronic structure of different conformations of the reaction participants.

Table 2. Geometric parameters of independent molecules of thiazaphospholine **IX**, obtained by quantum-chemical calculations

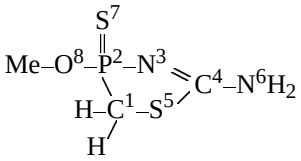

Parameter	MNDO	HF/6-31G*	MP2/6-31++G**	DFT
Bond		*d*, Å		
$P^2–C^1$	1.821	1.843	1.845	1.868
$P^2–N^3$	1.687	1.660	1.694	1.695
$N^3–C^4$	1.305	1.268	1.293	1.290
$C^4–S^5$	1.713	1.785	1.792	1.815
$C^4–N^6$	1.394	1.340	1.363	1.361
$C^1–S^5$	1.723	1.812	1.807	1.820
Bond angle		ω, deg		
$C^1P^2N^3$	100.4	100.7	100.6	100.8
$P^2N^3C^4$	113.4	115.9	113.4	114.5
$N^3C^4S^5$	120.7	121.9	123.2	122.6
$C^4S^5N^1$	98.5	94.6	94.0	94.4
$S^5C^1P^2$	107.0	106.8	107.6	107.3
Torsion angle		φ, deg		
$P^2N^3C^4S^5$	1.5	0.3	1.9	1.8
$N^3C^4S^5C^1$	1.1	2.2	5.1	2.9

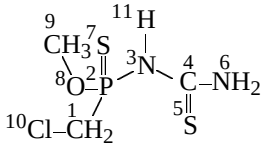

VIIa

Similar to all the phosphorylated ureas, *N*-(methoxychloromethylthiophosphoryl)thiourea **VIIa** is characterized by a large set of conformers differing in the torsion angles $C^1P^2–N^3C^4$, $P^2N^3–C^4S^5$, $Cl^{10}C^1–P^2N^3$, and $C^9O^8–P^2S^7$ corresponding to internal rotation about the four ordinary bonds $P^2–N^3$, $N^3–C^3$, $C^1–P^2$, and $P^2–O^8$ and in the orientation of the unshared electron pair of the nitrogen atom of the NH_2 group. The latter is described by the torsion angle $N^6C^4N^3H^{11}$. The heats of formation, the torsion angles, and one of the coordinates of the cyclization pathway, $C^1\cdots S^5$ distance, for the ten most characteristic stable conformers of **VIIa**, determined by the MNDO method, are presented in Table 3 together with the geometric characteristics of the most stable conformer obtained on the HF/6-31G* and DFT levels. Some conformers are additionally shown in Fig. 3.

Even a superficial consideration of the conformers shows that some of them (**VIIa**-1–**VIIa**-4) are sterically favorable for the initial nucleophilic attack of the carbon atom of the chloromethyl group with the sulfur atom, which may lead to the reaction products, thiazaphospholines **IXa**-1–**IXa**-4. In these conformers, the $C^1\cdots S$ distance is about 3 Å, the chlorine atom is drawn apart from the sulfur atom, and the $Cl^{10}C^1S^5$

Table 3. Heats of formation ΔH_f^0, torsion angles φ, and distances $d_{C^1–S^5}$ (Å) in the ten stable conformations of the independent molecule of *N*-(chloromethylthiophosphoryl)thiourea **VIIa** (MNDO method)

Conformation	ΔH_f^0, kJ mol^{-1}	φ, deg					$d_{C^1–S^5}$, Å
		$C^4N^3P^2C^1$	$S^5C^4N^3P$	$C^9O^8P^2S^7$	$Cl^{10}C^1P^2N^3$	$H^{11}N^3C^4N^3$	
1	–98.33	–61	36	–16	–170	–31	3.38
1[a]		–60	4	47	180	7	3.57
1[b]		–59	9	–42	–159	2	3.48
2	–79.90	–42	33	166	–176	30	3.34
3	–97.32	–52	10	–17	–170	35	3.37
4	–87.11	83	–36	–4	164	34	3.50
5	–88.16	83	–29	–14	47	35	3.58
6	–96.65	83	–177	–24	47	45	5.03
7	–96.19	172	160	–11	57	–36	5.29
8	–96.86	147	116	–19	54	24	5.38
9	–95.40	144	119	–12	174	25	5.33
10	–76.19	163	117	167	48	22	5.35

[a] HF/6-31G* method. [b] DFT method.

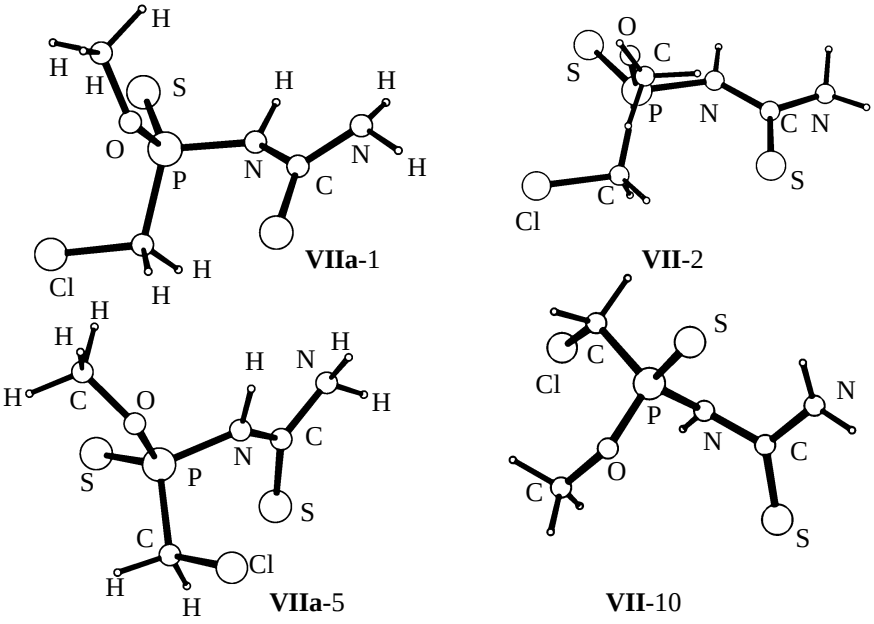

Fig. 3. Examples of the favorable (**VIIa**-1, **VIIa**-2) and unfavorable (**VIIa**-5, **VIIa**-10) conformations of thiourea **VIIa**.

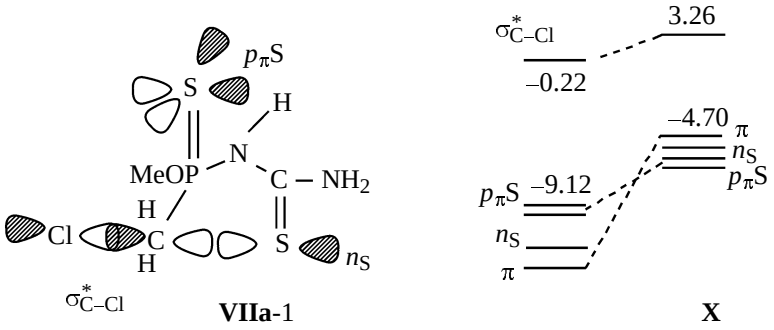

Fig. 4. Orbital characteristics of conformer **VIIa**-1 and anion **X**.

angle is close to 180°, which is favorable for the classic SN2 reaction. Some of other conformers of **VIIa** are clearly unfavorable for the alkylation of the thionic sulfur atom. In conformers **VIIa**-6–**VIIa**-10, the C and S atoms are separated in space (the $C^1 \cdots S$ distance is more than 5 Å). In conformer **VIIa**-5, these atoms are drawn together, but the interaction of the C and S atoms is hindered by chlorine (the $Cl^{10}C^1S^5$ angle is acute). Conformers **VIIa**-6, **VIIa**-8, and **VIIa**-10 are favorable for the cyclization into the alternative products, diazaphospholidines **VIII**-6, **VIII**-8, **VIII**-10, but this reaction actually does not take place and therefore was not considered in this study. Note only that the degree of piramidality of the nitrogen atom in the NH_2 group is small, and its change, as well as the change in the orientation of the unshared electron pair of the nitrogen atom, i.e., in the sign of the $H^{12}N^6C^4N^3$ angle, only slightly affects the energy of the conformers.

Considering the electronic structure of **VIIa**, we should note that conformers **VIIa**-1–**VIIa**-10 significantly differ from each other in the dipole moments, and to a smaller extent in the charges on atoms and HOMO energies. The "twisted" structures **VIIa**-1–**VIIa**-5, favorable for the nucleophilic attack of the C^1 atom with the sulfur atom from the conformational viewpoint, are also characterized by the larger effective negative charge on the S^5 atom. In all the conformers **VIIa**-1–**VIIa**-10, the HOMO Ψ_1 and the next occupied orbital Ψ_2 are localized on the S^7 atom of the thiophosphoryl group (in Fig. 4 they are marked as $p_\pi S$); the difference in the energy of these orbitals is about 0.1 eV, which is in good agreement with the published photoelectron spectra of the thiophosphoryl compounds, in which these orbitalas usually are not resolved [7–9]. The next two orbitals are the orbital of the unshared electron pair of thiocarbonyl sulfur $\Psi_3(n_S)$ and the π orbital of the thiocarbonyl bond

$\Psi_4(\pi)$. Note that the experimental ionization energies of the orbitals of the unshared electron pairs of the sulfur atom in thiophosphoryl and thiocarbonyl groups are close [7–9]. For example, the ionization potentials of these orbitals in the molecules of Me_3PS, Me_2CS, and $(H_2N)_2CS$ are 8.48, 8.60, and 8.50 eV, respectively [9, 10]. According to MNDO calculations, the orbital energies of the unshared electron pairs of the sulfur atom in the thiophosphoryl and thiocarbonyl groups in **VIIa** are also fairly close. For example, in conformer **VIIa**-1 they are –9.12 [$\Psi_1(p_\pi S)$] and –9.56 eV [$\Psi_3(n_S)$].[1] The energy of the antibonding orbital, localized to a considerable extent on the C–Cl bond, is –0.22 eV in this conformer.

Let us consider now the structure of the thiourea anion, transition states (TS), and reaction products, and also the shapes of the potential energy surfaces. In general, the energy profile of the cyclization must be fairly complicated, because it includes the rupture and formation of several bonds: The C^1–Cl, N^3–H, and C^4=S^5 bonds are cleaved, whereas the C^1–S^5 and N^3=C^4 bonds are formed. Also, the eliminated fragments (H, Cl) get bound with each other and can be coordinated by a base. In such an asymmetrical molecule as **VIIa**, these processes are hardly concerted. At the same time, it can be expected that, as in other similar reactions [11–13], the cyclization has significant features of SN2 reactions. The calculations have confirmed this assumption. Formation of a bond between the internal nucleophile (S or N atom) and the reaction center (saturated C^1 carbon atom) and the displacement of the nucleofugic group (Cl^{10} atom) are lagrely concerted. Considering that the cyclization proceeds only in the presence of bases, we have simulated two boundary cases in our study. In the first case, the starting thiourea is rapidly deprotonated, and the limiting step is the nucleophilic attack of the C^1 carbon atom with the sulfur atom of the resulting anion. In the second case, the intramolecular nucleophilic attack proceeds in the first, limiting step, and the subsequent dehydrohalogenation is fast.

As the cyclizations were carried out in the presence of an equimolar amount of a base, we believed the two-step process to be quite plausible from the very beginning. In the first step, the molecule of **VIIa** undergoes fast deprotonation to form anion **X**, and in the second, limiting step, the S^5 atom of the thiourea moiety nucleophilically attacks the C^1 atom of the chloromethyl group with the simultaneous displacement of the chlorine atom. Under these conditions, apparently, the anion forms cyclic transition state TS1 which subsequently tranforms into ion–molecule complex **XI** as the primary reaction product.[2]

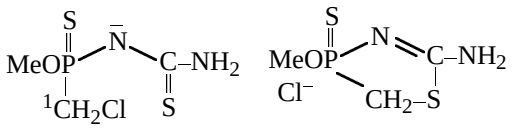

X **XI**

After that, complex **XI** decomposes to give the neutral cyclic product **IXa** and the chloride anion.

Anion **X**, as well as the starting thiourea, can exist in several conformations. The anion that we discuss below was calculated by all the above-mentioned quantum-chemical methods. It is the most similar in the structure to the favorable starting conformer **VIIa**-1 (Tables 4–6). Anion **X** is characterized by elongation of the C=S bond, accumulation of the negative charge on the sulfur atom, a significant increase in the HOMO level, and a decrease in the energy gap between the frontier orbitals as compared to the neutral molecule. All the calculation methods similarly reproduce an increase in the HOMO level [$\Delta\varepsilon_{HOMO}$, eV: 4.38 (MNDO), 4.67 (HF/6-31G*), 4.44 (DFT)]. The scatter in the LUMO energies is considerably larger; the energy gap between the frontier orbitals varies in going from the neutral molecule to the anion from 5.22 to 3.19 eV according to DFT calculations.

On the pathway from anion **X** to the ion–molecule complex, we, indeed, localized with all the three methods the transition state (the saddle point TS1) with the expected geometric characteristics (Tables 4, 5; Fig. 5). Its conformation is close to rthat of a planar five-membered ring and is characterized by elongation of the C^1–C^{10}, C^1–P^2, and C^4–S^5 bonds and by shortening of the C^4–N^3 bond, as compared to the starting acyclic structures (the neutral molecule and the anion). In the preceding anionic form, all the changes are considerably weaker. Shortening of the C^4–N^3 bond, which is double in the final phosphacyclane, shows that the order of this bond increases already in the transition state. Using the internal coordinate method, we realized a smooth descent from this saddle point to the valleys of both the reactants products, which characterizes this pathway as quite probable. Although in the gas phase the deprotonation is energetically hindered, the enthalpy of the reaction

[1] The energies of the occupied frontier orbitals obtained by other methods are also close.

[2] Among several ion–molecule complexes similar in the structure and energy (shallow minima on the bottom of a deep potential well), we consider only one of them, which was found to be the most stable according to the calculations.

Table 4. Energy characteristics and torsion angles (φ) in the independent molecules of the starting reactants, reaction products, and intermediates

Compound	Calculation method	E [b]	φ, deg			
			$C^4N^3P^2C^1$	$S^5C^4N^3P^2$	$C^9O^8P^2S^7$	$Cl^{10}C^1P^2N^3$
VIIa	MNDO	–98.33	–61	36	–16	–170
	HF/6-31G*	–1897.300098	–60	4	47	180
	DFT	–1901.024445	–59	9	–43	–179
IXa	MNDO	– 87.94	1	0	–29	–18
	HF/6-31G*	–1437.236804	–2.5	0.3	–53	–8
	DFT	–1440.391631	–3.1	1.1	–42	–12
X	MNDO	–332.4	–37	–3	–34	–174
	HF/6-31G*	–1896.770295	–59	–4	–70	178
	DFT	–1900.501397	–52	2	–56	180
TS1	MNDO	–241.6	10	–4	0	169
	HF/6-31G*	–1896.734046	28	–8	18	153
	DFT	–1900.488494	32	–8	26	154
XI	MNDO	–362.6	1	0	–44	–131
	HF/6-31G*	–1896.788373	10	–2	–55	–131
	DFT	–1900.522955	10	–2	–54	–133
TS2	MNDO	45.23	0	0	13	178
	HF/6-31G*	–1897.231513	31	–17	169	156
	DTF	–1900.989575	29	–19	170	170
XII	MNDO	–150.2	–102	59	158	–132
	HF/6-31G*	–1897.277082	–98	–99	180	–124
	DFT	–1901.023785	–91	53	179	–122

[a] The only negative frequences in each saddle point are as follows (cm^{-1}): TS1, –558 (MNDO), –509 (HF/6-31G*), –364 (DFT); TS2, –493 (MNDO), –563 (HF/6-31G*), –383 (DFT). [b] For MNDO, we present the heats of formation (ΔH_f^0, kJ mol^{-1}), and for HF/6-31G* and DFT, the total energies (au).

Table 5. Interatomic distances (d, Å) in structures and transition states corresponding to stationary points on the energy profiles of the cyclization **VIIa** → **X** → TS1 → **XI** → **IXa** and rearrangement **VIIa** → TS2 → **XII**

Compound	C^1–P^2	P^2–N^3	N^3–C^4	C^4–S^5	C^4–N^6	C^1–S^5	C^1–Cl^{10}	P^2=S^7	P^2–O^8	P^2–Cl^{10}
Cyclization **VIIa** → **X** → TS1 → **XI** → **IXa**										
VIIa-1	1.814	1.684	1.397	1.580	1.402	3.381	1.776	1.923	1.611	2.925
	1.821	1.712	1.366	1.672	1.334	3.569	1.786	1.936	1.569	2.988
	1.841	1.742	1.384	1.675	1.369	3.484	1.795	1.950	1.623	3.001
X	1.810	1.641	1.336	1.612	1.428	3.351	1.794	1.931	1.633	3.000
	1.835	1.613	1.311	1.728	1.359	3.636	1.792	1.968	1.604	3.072
	1.853	1.649	1.337	1.720	1.394	3.453	1.815	1.981	1.664	3.104
TS1	1.836	1.684	1.313	1.653	1.414	2.084	2.068	1.926	1.625	2.901
	1.857	1.640	1.284	1.743	1.358	2.460	2.374	1.955	1.588	3.295
	1.854	1.685	1.306	1.753	1.389	2.450	2.294	1.975	1.647	3.238
XI	1.817	1.695	1.303	1.705	1.408	1.724	3.288	1.918	1.615	4.345
	1.838	1.557	1.267	1.776	1.354	1.815	3.540	1.951	1.584	4.638
	1.855	1.705	1.291	1.798	1.378	1.822	3.312	1.966	1.635	4.414
IX	1.821	1.687	1.305	1.713	1.394	1.723	–	1.913	1.614	–
	1.843	1.660	1.268	1.785	1.340	1.812	–	1.936	1.595	–
	1.868	1.694	1.290	1.815	1.361	1.819	–	1.949	1.6471	–

Table 5. (Contd.)

Compound	C^1–P^2	P^2–N^3	N^3–C^4	C^4–S^5	C^4–N^6	C^1–S^5	C^1–Cl^{10}	P^2=S^7	P^2–O^8	P^2–Cl^{10}
Rearrangement **VIIa** → TS2 → **XII**										
TS2	1.857	1.754	1.347	1.649	1.3632	1.953	2.083	1.909	1.609	2.549
	1.830	1.761	1.326	1.704	1.322	2.286	2.428	1.913	1.565	3.021
	1.823	1.809	1.339	1.710	1.356	2.305	2.356	1.933	1.625	2.842
XII	1.820	4.062	1.291	1.707	1.417	1.709	3.065	1.896	1.607	2.046
	1.831	4.480	1.250	1.815	1.367	1.815	2.972	1.917	1.577	2.076
	1.856	4.396	1.275	1.847	1.375	1.822	3.025	1.928	1.631	2.121

Table 6. Effective charges[a] on the atoms of stationary states on the pathways of cyclization **VIIa** → **X** → TS1 → **XI** → **IXa** and rearrangement **VIIa** → TS2 → **XII**, according to different calculation methods

Compound	Method	C^1	P^2	N^3	C^4	S^5	N^6	Cl^{10}
Cyclization **X** → **IXa**								
VIIa-1	MNDO	0.045	0.756	0.492	0.182	–0.192	0.294	–0.118
	HF/6-31G*	–0.658	1.285	–0.942	0.481	–0.314	–0.865	–0.036
	DFT	–0.083	0.373	–0.148	0.090	–0.227	–0.152	–0.044
X	MNDO	0.007	0.754	0.552	0.178	–0.482	0.264	–0.207
	HF/6-31G*	–0.647	1.275	–0.791	0.416	–0.538	–0.844	–0.124
	DFT	–0.096	0.332	–0.284	0.064	–0.396	–0.199	–0.122
TS1	MNDO	0.222	0.671	0.445	0.110	–0.350	0.239	–0.631
	HF/6-31G*	–0.488	1.227	–0.693	0.381	–0.372	–0.853	–0.682
	DFT	–0.088	0.332	–0.277	0.067	–0.365	–0.193	–0.367
IXa	MNDO	–0.235	0.676	0.384	0.078	0.180	0.232	
	HF/6-31G*	–0.786	1.180	–0.667	0.384	0.197	0.876	
	DFT	–0.116	0.355	–0.244	0.094	0.020	–0.153	
Rearrangement **VII** → **XII**								
TS2	MNDO	0.211	0.744	–0.473	0.246	–0.107	–0.310	–0.578
	HF/6-31G*	–0.621	1.291	–0.898	0.488	–0.078	–0.862	–0.635
	DFT	–0.087	0.362	–0.140	0.105	–0.248	–0.138	–0.333
XII	MNDO	–0.210	0.765	–0.472	0.098	0.458	–0.278	–0.577
	HF/6-31G*	–0.773	1.035	–0.849	0.341	0.179	–0.674	–0.239
	DFT	–0.125	0.322	–0.166	0.089	0.045	–0.262	–0.059

[a] In the electron charge units.

in solution may be decreased owing to the effects of solvation and formation of a tight ion pair with a base, or to the incomplete proton transfer of proton in the solvated complex.

Then we attempted to reach the similar complex via transition state TS2 taking as the starting point conformer **VIIa**-1, which is the most favorable sterically and electronically. Under these conditions, we expected to obtain an *a fortiori* higher activation barrier than in the above-described case, taking into account the difference in the electronic structure of the anion and the neutral molecule of similar geometry (Tables 5, 6). We, indeed, revealed a saddle point TS2 on the reaction pathway (Fig. 5) lying higher than the starting reactants (Table 4). A descent from TS2 to the valley of reactants was regular in all the cases (the conformational characteristics of the thiourea naturally differed from each other), whereas the descent to the valley of products unexpectedly led not to cyclic product **IXa** or the corresponding ion pair, but to cyclic product **XII**. In this structure, the chlorine atom is bound to phosphorus, i.e., point TS2 appeared to be the saddle point of structural isomerization.

Different calculation procedures give different

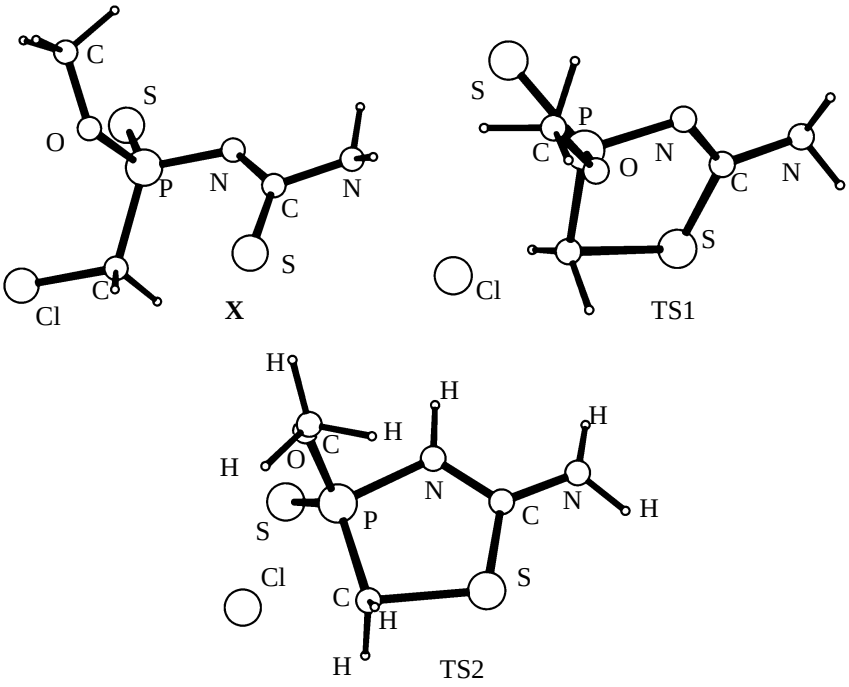

Fig. 5. Steric structure of anion **X** and saddle points TS1 and TS2.

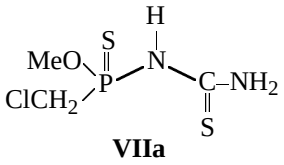

VIIa

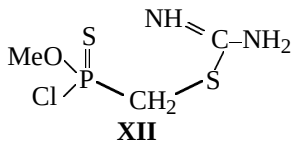

XII

orders of stability of structures **VII** and **XII**. The MNDO data show that structure **XII** is more stable than **VII**, whereas more rigorous calculations show that structure **XII** is less stable than **VII** (Table 4).

To characterize the saddle point TS2 in more detail, the heterocyclic fragment of this structure is almost planar, the Cl^{10}–C^1–S^5 fragment is almost linear, and the torsion angle $Cl^{10}C^1P^2N^3$ is close to 180°C, which corresponds to the usual transition states in intramolecular nucleophilic substitutions [13]. The transition state TS2 is characterized by significant charge transfer to the chlorine atom from the atoms of the cyclic fragment and by the elongation of the P^2–N^3 bond.

Detailed analysis of changes in the geometry in the course of the ascent and descent shows that the formation of the S^5–C^1 bond is the fastest step. The chlorine atom of the anion moves apart simultaneously from the carbon and phosphorus atoms, i.e., it leaves the chemical particle. In the neutral molecule, the chlorine atom moves between the carbon and phosphorus atoms. As the chlorine atom approaches the phosphorus atom, the P–N bond weakens and finally is broken. Note that the rearrangement product may also lead to thiazaphospholine **IXa** by displacement of the chlorine atom in **XII** from the phosphorus atom in the course of the nucleophilic attack of the latter by the N^3 atom, which, however, requires overcoming of one more potential barrier.

Considering the activation characteristics of the cyclization of the anion [transition from anion **X** to saddle point TS1, i.e., process (1)] and the structural rearrangement of the most favorable conformer of the neutral molecule [transition from conformer **VIIa**-1 to saddle point TS2, i.e., process (2)], we should note that, according to the results furnished by all the calculation methods, in both processes the activation enthalpy and entropy (298.15 K) are negative. The activation free energy ($\Delta G^{\neq}$, kcal mol^{-1}) of the first process is significantly lower than that of the second process.

	HF/6-31G*	DFT
Process (1)	23.1	9.3
Process (2)	43.7	22.9

These data show that the consideration of the electronic correlation significantly decreases the activation barriers in both cases.

The difference in the activation parameters can be well explained by the above-mentioned differences in the electronic structure of the reagents, in spite of their similar geometric characteristics.

To sum up, it should be admitted that the actual reaction pathway is complex and, along with the major gradient pathway, it apparently involves side pathways [13], which is largely due to the conformational lability of the system. Comparison of the experimental and theoretical data suggests that the most probable reaction pathway can be described as follows. First, a complex between the base (triethylamine) and thiourea **VIIa** is formed. The complexation weakens the N^3–H bond (according to MNDO calculations, this interatomic distance in the H-complex is 1.032 Å, whereas in **VIIa** it is 1.006Å), and even an ion pair $X^-Et_3NH^+$ may form. That is, the pattern is close to the first of the cases considered. The $C^1\cdots S$ bond in the reaction complex is formed before the rupture of the $C^1\cdots Cl$ bond. On the qualitative level, the structure of the reagents, intermediates, transition states, and products is satisfactorily described by both *ab initio* and semiempirical methods. To judge the correctness of the energy characteristics, the reliable thermochemical and kinetic data should be obtained. Today such data are lacking.

EXPERIMENTAL

The IR spectra were recorded on a UR-20 spectrometer in the range 400–3600 cm^{-1} (mulls in mineral oil or thin films). The ^{31}P NMR spectra were taken on a Bruker MSL-400 NMR Fourier spectrometer (161.97 MHz) and on a KGU-4 NMR spectrometer (10.2 MHz) against external 85% phosphoric acid. The ^1H NMR spectra were measured on Bruker WM-250 (250.132 MHz) and Varian T-60 (60 MHz) spectrometers against internal TMS.

Single crystal X-ray diffraction analysis of III. The unit cell parameters and intensities of 2327 reflections, including 1677 reflections with $I > 3\sigma$, were measured on an Enraf-Nonius CAD-4 automatic four-circle diffractometer at 20°C (λMoK_α radiation, graphite monochromator, $\omega/2\theta$-scanning, $\theta \le 26.9°$). No decrease in the intensity of three check reflections in the course of the experiment was observed; the absorption was neglected (μMo 3.58 cm^{-1}). Monoclinic crystals, unit cell parameters at 20°C: *a* 11.835(2), *b* 9.487(1), *c* 17.099(3) Å; β 90.02(1)°, *V* 1919.9(5) $Å^3$, *Z* 4, d_{calc} 1.32 g cm^{-3}, space group $P2_1/a$. As the monoclinic angle is equal to 90° within the experimental error, the crystal was initially assigned to the rhombic system, but checking of its point group (by convergence of rhombic equivalents) showed that actually it is monoclinic. The space group of the crystal was established from systematic absences, which also confirm the monoclinic type of the crystal. The structure was solved by the direct method using the SIR program [14] and refined first in the isotropic and then in the anisotropic approximation. After that, all the hydrogen atoms were revealed from the differential electron density series and were refined isotropically in the final step. The structure was refined to *R* 0.033 and R_W 0.046 for 1635 unique reflections with $F^2 > 3\sigma$. All the computations were carried out with a DEC Alpha Station 200 computer using the MolEN software [15]. The analysis of intermolecular contacts in the crystal and the drawings of the molecule and the crystal structure were made using the PLATON program [16]. The calculations were carried out using the MOPAC [17], GAMESS [18], and PRIRODA [19] programs. Complete optimization of the geometry of the molecular structures corresponding to the energy minima ($\lambda = 0$, λ is the number of eigenvalues of the Hesse matrix in the given stationary point) and saddle points ($\lambda = 1$) on the potential energy surface of the system was carried out to the gradient value of 10^{-5} au $bohr^{-1}$. The structures corresponding to the energy minima on the potential energy surface were found by the steepest descent (moving along the gradient line) from the saddle point (TS) to the neighboring stationary point. The initial direction of the gradient line was given by a small displacement along the transition vector.

2-(1,1,3,3-Tetramethyl)guanidino-4-thioxo-4-phenoxy-Δ^2-1,3,4λ^5-thiazaphospholine III. A 1.85-g portion of *O*-phenyl chloromethylisothiocyanatidophosphonothioate **I** was added dropwise with stirring at 5°C to a solution of 0.81 g of tetramethylguanidine and 1 g of triethylamine in 50 ml of anhydrous benzene. The mixture was left overnight, after which triethylamine hydrochloride was filtered off, and the filtrate was washed with water (3 × 5 ml) and dried over anhydrous sodium sulfate. Then the solvent was removed, and 1.5 g (63%) of **III** was obtained by crystallization from hexane, mp 109–111°C. IR spectrum (KBr), ν, cm^{-1}: 1195 (Ph), 1570 ($C=N_{endo}$), 1590 (Ph), 1660 ($C=N_{exo}$). ^1H NMR spectrum ($CDCl_3$), δ, ppm: 2.85 s (12H, CH_3N); 3.48 m, 3.68 m (2H, CH_2P, $^2J_{PH_A} = {}^2J_{H_AH_B}$ 13.2, $^2J_{PH_B}$ 4.4 Hz), 7.22 m (5H, Ph). ^{13}C NMR spectrum ($CDCl_3$), δ_C, ppm: 40.18 q.q (C^9, C^{10}, C^{12}, C^{13}, $^1J_{CH}$ 137.1 Hz, $^3J_{CH}$ 3.4 Hz), 166.0 m (C^7), 173.8 m (C^2), 36.2 (d.) d.d (C^5, $^1J_{PC}$ 52.0, $^1J_{CH_A}$ 144.0, $^1J_{CH_B}$ 147.0 Hz), 151.2 d.m (C^{15}, $^2J_{PC}$ 10.5 Hz), 121.2 m (C^{16}, $^1J_{CH}$ 162.0, $^3J_{PC}$ 4.7, $^3J_{CH}$ 4.5 Hz), 129.1 d.d (C^{17}, $^1J_{CH}$ 162.0, $^3J_{CH}$ 8.3 Hz), 124.2 m (C^{18}, $^1J_{CH}$ 163.0, $^3J_{PC}$ 7.0, $^5J_{CH}$ 7.0 Hz). ^{31}P NMR spectrum: δ_P 118 ppm. Found, %: C 45.47; H 5.71; N 16.26; P 9.24; S 18.36. $C_{13}H_{19}N_4OPS_2$. Calculated, %: C 45.59; H 5.60; N 16.36; P 9.04; S 18.72.

***N,N'*-Di(4-thioxo-4-phenoxy-Δ^2-1,3,4λ^5-thiazaphospholin-2-yl)ethylenediamine VIa** was prepared similarly from 2 g of isothiocyanate **I**, 1.1 g of triethylamine, and 0.23 g of ethylenediamine **IVa**. Yield 1.15 g (60%), mp 50–53°C. IR spectrum (KBr), ν, cm^{-1}: 1200 (PhOP), 1565 (C=N), 1590 (Ph), 3240 (NH). ^1H NMR spectrum ($CDCl_3$), δ, ppm: 3.62 m (8H, CH_2P, CH_2N), 7.28 m (10H, Ph), 9.06 br.s (2H, NH). ^{31}P NMR spectrum, δ_P, ppm: 119.5. Found, %: C 41.61; H 4.00; N 10.80; P 12.53. $C_{18}H_{20}N_4O_2P_2S_4$. Calculated, %: C 42.01; H 3.93; N 10.89; P 12.04.

2-Methyl-*N,N'*-di(4-thioxo-4-phenoxy-Δ^2-1,3,4λ^5-thiazaphospholin-2-yl)ethylenediamine VIb was prepared similarly from 3.0 g of isothiocyanate **I**, 1.6 g of triethylamine, and 0.42 g of 1,2-propanediamine **IVb**. Crystallization from chloroform gave 2.1 g (87%) of **VIb**, mp 55–57°C. IR spectrum (KBr), ν, cm^{-1}: 1200 (PhOP), 1565 (C=N), 1590 (Ph), 3240 (NH). ^1H NMR spectrum ($CDCl_3$), δ, ppm: 1.45 m (3H, CH_3C); 2.97–4.23 m (7H, CH_2P, CH_2N, CHN); 7.45 m (10H, Ph). ^{31}P NMR spectrum, δ_P, ppm: 117.6, 116.8; 117.5, 116.7; 117.7, 116.5; 117.0, 116.3. Found, %: C 43.22; H 4.39; N 10.13; P 11.50; S 23.83. $C_{19}H_{22}N_4O_2P_2S_4$. Calculated, %: C 43.17; H 4.20; N 10.60; P 11.72; S 24.26.

ACKNOWLEDGMENTS

The study was financially supported by the Russian Foundation for Basic Research (project no. 03-03-33064).

REFERENCES

1. Kamalov, R.M., Khailova, N.A., Gazikasheva, A.A., Chertanova, L.F., Pudovik, M.A., and Pudovik, A.N., *Dokl. Akad. Nauk SSSR*, 1991, vol. 306, no. 6, p. 1406.
2. Pudovik, M.A., Saakyan, G.M., Khairullin, V.K., Khailova, N.A., and Pudovik, A.N., *Izv. Ross. Akad. Nauk, Ser. Khim.*, 1999, no. 4, p. 810.
3. Khailova, N.A., Krepysheva, N.E., Saakyan, G.M., Bagautdinova, R.Kh., Shaimardanova, A.A., Zyablikova, T.A., Azancheev, N.M., Litvinov, I.A., Gubaidullin, A.T., Zverev, V.V., Pudovik, M.A., and Pudovik, A.N., *Zh. Obshch. Khim.*, 2002, vol. 72, no. 7, p. 1145.
4. Khailova, N.A., Shaimardanova, A.A., Avvakumova, L.V., Shagidullin, R.R., Pudovik, M.A., Zverev, V.V., and Pudovik, A.N., *Zh. Obshch. Khim.*, 2000, vol. 70, no. 2, p. 247.
5. Chmutova, G.A., Zverev, V.V., Pudovik, M.A., Khailova, N.A., and Pudovik, A.N., *Zh. Obshch. Khim.*, 2003, vol. 73, no. 11, p. 1793.
6. Khailova, N.A., Shaimardanova, A.A., Saakyan, G.M., Zyablikova, T.A., Azancheev, N.M., Krivolapov, D.B., Gubaidullin, A.T., Litvinov, I.A., Musin, R.Z., Chmutova, G.A., Pudovik, M.A., and Pudovik, A.N., *Zh. Obshch. Khim.*, 2003, vol. 73, no. 8, p. 1284.
7. Zverev, V.V., Vilesov, F.I., Vovna, V.I., Lopatoi, S.N., and Kitaev, Yu.P., *Izv. Akad. Nauk SSSR, Ser. Khim.*, 1975, no. 5, p. 1051.
8. Zverev, V.V., Villem, Ya.Ya., Liorber, B.G., and Kitaev, Yu.P., *Zh. Obshch. Khim.*, 1981, vol. 51, no. 2, p. 303.
9. Nefedov, V.I. and Vovna, V.I., *Elektronnaya struktura organicheskikh i elementoorganicheskikh soedinenii* (Electronic Structure of Organic and Heteroorganic Compounds), Moscow: Nauka, 1989, pp. 189–190.
10. Rao, C.N.R., Basu, P.K., and Hegde, M.S., *Appl. Spectrosc. Rev.*, 1979, vol. 15, no. 1, p. 1.
11. Palm, V.A., *Vvedenie v teoreticheskuyu organicheskuyu khimiyu* (Introduction to Theoretical Organic Chemistry), Moscow: Vysshaya Shkola, 1974, p. 305.
12. March, J., *Advanced Organic Chemistry. Reactions, Mechanisms, and Structure*, New York: Wiley, 1982, 3rd ed. Translated under the title *Organicheskaya khimiya*, Moscow: Mir, 1987, vol. 2, p. 504.
13. Minyaev, R.M., *Usp. Khim.*, 1994, vol. 63, no. 11, p. 939.
14. Altomare, A., Cascarano, G., Giacovazzo, C., and Viterbo, D., *Acta Crystallogr., Sect. A*, 1991, vol. 47, p. 744.
15. Straver, L.H. and Schierbeek, A.J., *MolEN. Structure Determination System*, Nonius B.V., 1994, vols. 1, 2.
16. Speek, A.L., *Acta Crystallogr., Sect. A*, 1990, vol. 46, no. 1, p. 34.
17. Stewart, J.J.P., MOPAC, Ver. 6.12.QCPE 455, Bloomington: Indiana Univ., 1990.
18. Schmidt, M.W., Baldridge, K.K., Boatz, J.A., Elbert, S.T., Gordon, M.S., Jensen, J.H., Koseki, S., Matsunaga, N., Nguyen, K.A., Su, S.J., Mindus, T.L., Dupnis, M., and Montgomeri, J.A., *J. Comput. Chem.*, 1993, vol. 14, no. 11, p. 1347.
19. Laikov, D.N., *Chem. Phys. Lett.*, 1997, vol. 281, p. 151.